JOURNAL OF GEOPHYSICAL RESEARCH, VOL. 100, NO. D7, PAGES 13,939–13,950, JULY 20, 1995

Formation of low-ozone pockets in the middle stratospheric anticyclone during winter

G. L. Manney,[1] L. Froidevaux,[1] J. W. Waters,[1] R. W. Zurek,[1] J. C. Gille,[2] J. B. Kumer,[3] J. L. Mergenthaler,[3] A. E. Roche,[3] A. O'Neill,[4] R. Swinbank[5]

Abstract. Microwave limb sounder observations of midstratospheric ozone during stratospheric warmings show tongues of high ozone drawn up from low latitudes into the developing anticyclone. Several days later, an isolated pocket of low ozone mixing ratios appears, centered in the anticyclone, and extending in the vertical from ≈15 to 5 hPa, with higher mixing ratios both above and below. These low ozone mixing ratios during northern hemisphere warmings are comparable to values well inside the vortex and are ≈3 parts per million by volume lower than typical midlatitude extra-vortex mixing ratios. This type of feature is seen whenever the anticyclone is strong and persistent, including during relatively strong minor warmings in the southern hemisphere. Three-dimensional back trajectory calculations indicate that the air in the region of the low-ozone pockets originates at higher altitudes and low latitudes, where ozone mixing ratios are much higher. The air parcels studied here are typically confined together for 1 to 3 weeks before the lowest ozone mixing ratios are observed. The trajectory calculations and comparisons with passive tracer data confirm that the observed low-ozone regions in the midstratosphere could not result solely from transport processes.

Introduction

The microwave limb sounder (MLS) instrument on the Upper Atmosphere Research Satellite (UARS) has measured ozone throughout the stratosphere since September 1991, through four northern hemisphere (NH) and three southern hemisphere (SH) winters [*Froidevaux et al.*, 1994]. This provides a multiyear data set of three-dimensional ozone fields, including measurements during many dynamically active periods in both hemispheres.

Strong stratospheric warmings are common throughout the NH winter [e.g., *Andrews et al.*, 1987], and weaker warmings are common in early and late winter in the SH [e.g., *Farrara et al.*, 1992; *Manney et al.*, 1993]. During these events the polar vortex is typically shifted off the pole and tongues of low-latitude air are seen to be drawn into the polar regions from low latitudes [e.g., *Manney et al.*, 1993, 1994a] in the midstratosphere. Planetary-scale waves are generally strongest in the middle and upper stratosphere [*Manney et al.*, 1991; *Fishbein et al.*, 1993], so the distortion and displacement of the vortex is greatest there. The shift of the vortex off the pole is associated with the formation of a large, strong anticyclone. In the NH an anticyclone, the "Aleutian high," persists through much of the winter [e.g., *Andrews et al.*, 1987]; during strong NH warmings this anticyclone may be as large as the polar vortex and may remain very strong for 10 to 15 days [e.g., *Manney et al.*, 1994a].

Examination of midstratospheric MLS ozone data during a number of stratospheric warmings reveals that while tongues of ozone rich air are drawn into the anticyclone from low latitudes during stratospheric warmings, this is followed by the formation of an isolated region of very low ozone in the anticyclone. We show here observed meteorological and ozone fields for several examples of this phenomenon. In addition, we use passive tracer data from MLS and the cryogen limb array etalon spectrometer (CLAES) on UARS and calculations of air parcel trajectories to explore the origins of the air in these low ozone regions.

Data and Analysis

The ozone data are from the MLS 205-GHz radiometer; they have a horizontal resolution of ≈400 km and an intrinsic vertical resolution of ≈4 km. The UARS MLS instrument is described by *Barath et al.* [1993], the

[1] Jet Propulsion Laboratory/California Institute of Technology, Pasadena, California

[2] National Center for Atmospheric Research, Boulder, Colorado

[3] Lockheed Palo Alto Research Laboratory, Palo Alto, California

[4] Centre for Global Atmospheric Modelling, Reading, England

[5] Meteorological Office, Bracknell, England

Paper number 95JD00372.
0148-0227/95/95JD-00372$05.00

measurement technique by *Waters* [1993], and retrieval methods by *Froidevaux et al.* [1994]. Precisions (rms) of individual ozone measurements for the altitudes examined here are ≈0.3 parts per million by volume (ppmv), with absolute accuracies of ≈5-15% [*Froidevaux et al.*, 1994].

Passive tracer data include water vapor (H_2O) from MLS and nitrous oxide (N_2O) and methane (CH_4) from CLAES. The CLAES instrument is described by *Roche et al.* [1993]. An earlier version of the CLAES N_2O and CH_4 data is described by *Kumer et al.* [1993]. The data are still in the validation process; this process has verified that the data used here (v0007) are suitable for studies of morphology and regional variation. Typical precision and systematic error estimates for N_2O in the midstratosphere are (10 parts per billion by volume (ppbv) rms, 20%), and for CH_4 are (50 ppbv, 20%). The MLS H_2O data are described by *Lahoz et al.* [1994]. Single profile precision and accuracy estimates for H_2O are (0.3 ppmv, 15%) at 4.6 hPa [*Lahoz et al.*, 1994]. Comparison of these passive tracer data with potential vorticity (PV) indicates that N_2O show the strongest correlation with PV at the levels and during the time periods discussed here; we therefore focus more closely on N_2O than on the other tracers.

Both CLAES and MLS data have been mapped to a 4°latitude by 5°longitude grid, consistent with the general meridional resolution of both instruments. CLAES data are gridded by linearly interpolating data for a 24-hour period to a regular latitude-longitude grid; ascending and descending orbit tracks are treated separately and then averaged. MLS data are gridded using Fourier transform techniques that separate time and longitude variations [*Elson and Froidevaux*, 1993]. All data are interpolated to isentropic (θ) surfaces using United Kingdom Meteorological Office (UKMO) temperatures.

The trajectory code used here is described by *Manney et al.* [1994b]; it uses a standard fourth-order Runge-Kutta scheme. Winds and temperatures are interpolated linearly in time from once daily values to the trajectory time step (1/2 hour). Heating rates are recalculated every 3 hours using interpolated temperatures and are interpolated linearly to the trajectory time step between calculations. Horizontal winds are from the UKMO data assimilation system [*Swinbank and O'Neill*, 1994] and vertical velocities from a recent version of the middle atmosphere radiation code MIDRAD, an earlier version of which is described by *Shine* [1987]. Temperatures in the radiation code are from the UKMO data; MLS ozone is used in the heating rate calculation, except for the December 1993 case, when MLS ozone measurements are not continuously available. *Manney et al.* [1994b] discuss the impact of using climatological versus MLS ozone.

The temperatures shown here are from the UKMO data, and Rossby-Ertel potential vorticity (PV) calculated from the UKMO data [*Manney and Zurek*, 1993] is also used.

MLS ozone data are available from September 1991 to the present. MLS H_2O and CLAES data are available through the 1992/1993 NH winter. Because of the UARS orbit, the data coverage switches from ≈34°S to 80°N to ≈80°S to 34°N approximately every 36 days. The examples examined here occur during late February and early March 1993, December 1992 and 1993 in the NH, and in the 1993 and 1994 SH winters.

Observed Characteristics

Plate 1 shows maps of 840 K ozone, with two PV contours overlaid, for three time periods in the NH winter. Stratospheric warmings during February and March 1993 were described by *Manney et al.* [1994a]; early winter warmings during December 1992 and 1993 are briefly described by *Manney et al.* [1994b]. The outermost PV contour shown on the ozone maps is along the outside of the region of strong gradients that coincide with the jet core; the innermost contour is in the middle of this region; these give an indication of the extent and shape of the polar vortex. In each of these time periods, tongues of relatively high ozone from low latitudes are drawn up around the polar vortex and into the region of the anticyclone which intensifies during stratospheric warmings (February 23, 1993; December 12, 1992; November 28, 1993). In the succeeding days, however, an isolated region of low ozone forms in the anticyclone, with ozone mixing ratios comparable to those well within the polar vortex (March 7, 1993; December 24, 1992; December 18, 1993). This region of low ozone may persist for some time; for example, the low ozone seen in the anticyclone on March 7, 1993, persists for over a week after that date, and mixing ratios become even lower.

Plate 2 displays the 840 K UKMO temperatures on the two days in December 1992, showing the typical relationship between the region of maximum temperatures and that of low ozone. In each of these events the maximum temperatures are seen near the time when tongues of high ozone are being drawn up around the vortex. The region of lower ozone forms to the eastward and equatorward side (downstream) of the region of highest temperatures, several days after the temperature maximum. *Remsberg et al.* [1994] showed that temperatures derived from nadir-viewing satellite data (as are the UKMO temperatures) could be signifcantly underestimated in the vicinity of the maximum temperatures. Examination of MLS temperatures for these days shows maximum values close to but slightly lower than those shown here.

Plate 3 shows the vertical structure of the pockets of low ozone. Profiles taken along the orbit tracks (i.e., prior to the gridding) are shown in the region of low ozone on a day when it is well developed. The green profiles in Plates 3b and 3c and the red profile in Plate 3a are near the edge of the region. The pressure levels labeled are the levels at which MLS data are currently retrieved. In general, the low ozone pocket appears as a bite out of the ozone profile in the altitude region of the mixing ratio peak, most prominent at the 10-hPa and 4.6-hPa retrieval levels. Ozone mixing ratios outside the

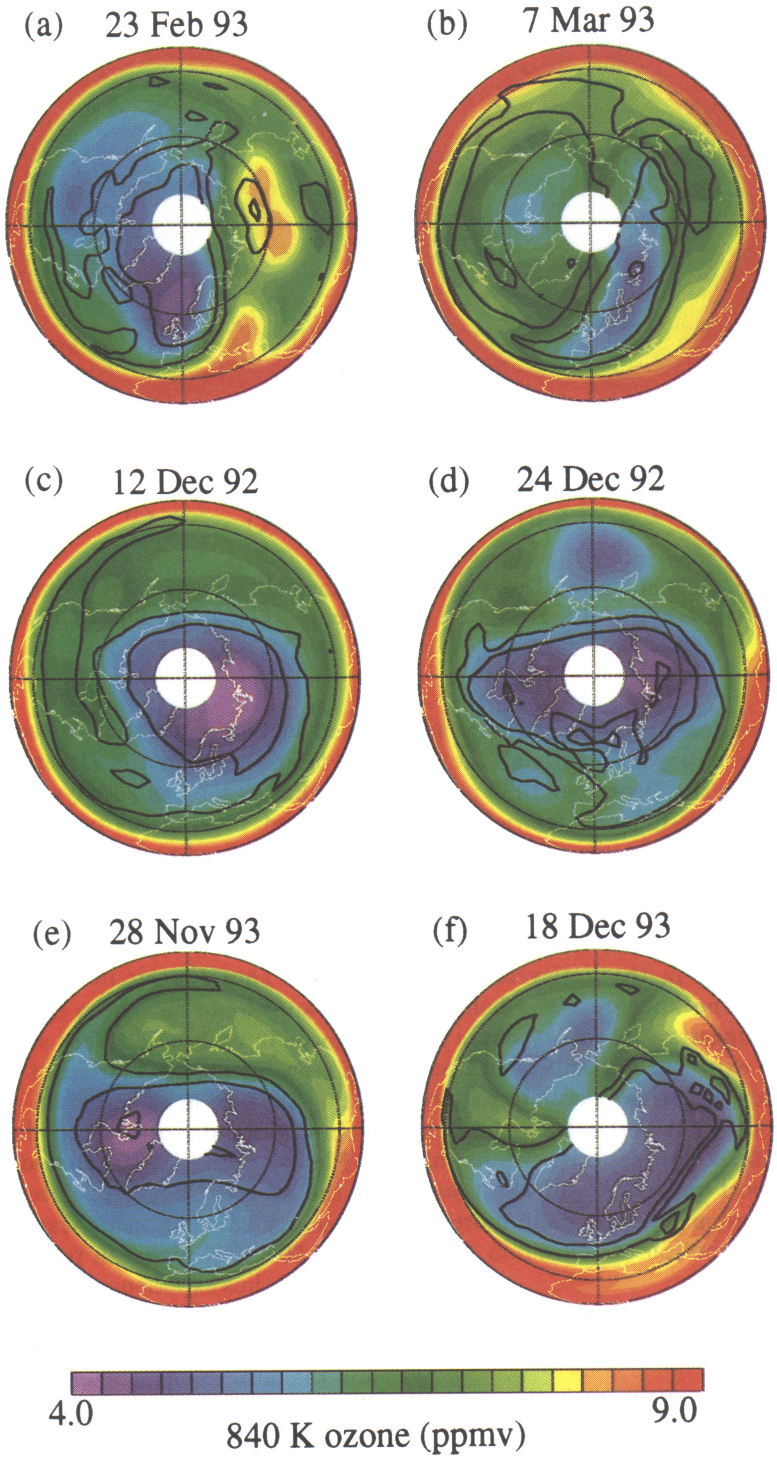

Plate 1. Synoptic maps of ozone mixing ratios (parts per million by volume (ppmv)) with overlaid potential vorticity (PV) contours at 840 K, in the northern hemisphere (NH), on (a) February 23, 1993, (b) March 7, 1993, (c) December 12, 1992, (d) December 24, 1992, (e) November 28, 1993 and (f) December 18, 1993. Overlaid PV contours at 840 K are 3.0 and 5.0×10^{-4} K m^2 kg^{-1} s^{-1}. Projection is orthographic, with 0°longitude at the bottom of the plot and 30 and 60°latitude circles shown as thin dashed lines.

vortex at these latitudes are typically near 8 ppmv [e.g., *Froidevaux et al.*, 1994] even when higher ozone is not drawn up from low latitudes, so these pockets represent a decrease in ozone that is in some cases over 3 ppmv. Similar features are also apparent in the CLAES ozone data during periods when they are available.

The 840 K N_2O maps for the February/March 1993 period [*Manney et al.*, 1994a] show a tongue of high

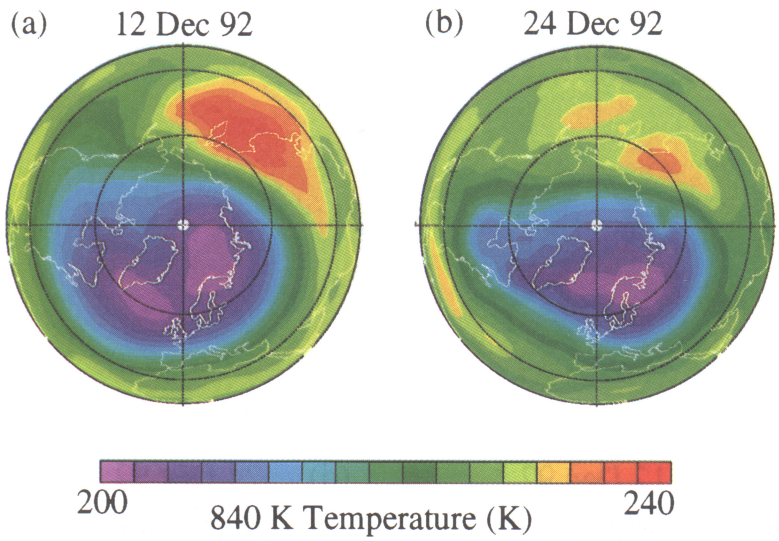

Plate 2. Synoptic maps of United Kingdom Meteorological Office (UKMO) temperatures at 840 K in the NH on (a) December 12, 1992; and (b) December 24, 1992. Layout is as in Plate 1.

N_2O drawn into the anticyclone from low latitudes and high N_2O persisting in the anticyclone through the period. Similar N_2O maps for the December 1992 period (not shown) again show high N_2O being drawn in from low latitudes and persisting in the anticyclone; maps of CLAES CH_4 show similar features. The 840 K maps of MLS H_2O for December 1992 and February/March 1993 (not shown) show a tongue of low H_2O drawn in from low latitudes persisting in the anticyclone during the time when low ozone appears. The behavior of these passive tracers suggests that low ozone in the anticyclone might not be expected to result from transport processes alone. However, this postulate requires further study since the different vertical and horizontal gradients of each of these trace species means that three-dimensional transport processes will affect each differently. In the next section we examine in more detail the three-dimensional motion of the air in which regions of low ozone form.

Diagnosis of Air Motion

To examine the origin of the air with low ozone mixing ratios in the anticyclone, we have initialized a number of parcels (between 3200 and 3840 per level in each case) on several isentropic surfaces in the midstratosphere, in the region of low ozone, and run 22 day back trajectory calculations (back to near the beginning of the period when MLS began looking north). Plate 4 shows the initial positions of parcels started at 840 K, and their positions 20 days earlier for each of the three events. The parcels are color coded by the observed ozone at their positions on the plotted day, and the same 840 K PV contours shown in Plate 1 are overlaid to indicate the position of the polar vortex. In each case, the trajectory calculation suggests that most or all of the parcels originated at lower latitudes in a region of much higher ozone than is seen in the anticyclone at the later time. In the December 1993 case it can be seen that as long as 20 days before the calculation was initialized, most of the parcels are grouped together in a fairly localized area. This event was the most persistent of those shown here, but in fact, examination of the other cases 10 days before the initialization (not shown) shows most of the parcels grouped together in a small region. Thus the air in which the low-ozone pockets form appears to have been confined together for a week or more in each case. Very similar horizontal motions are seen for parcels started at 740 K and 960 K, indicating that air is being drawn up from low latitudes in a similar manner over a deep layer.

Plate 5 shows the calculated potential temperatures of the parcels 20 days before the initialization. The trajectory calculation indicates that the parcels originated 60-140 K higher in potential temperature at that time and thus experienced diabatic descent from ≈3 to 7 K/d. The strongest diabatic descent rates during stratospheric warmings are in the region between the vortex and the anticyclone, coincident with the region of highest temperatures [e.g., *Manney et al.*, 1994a]. In moving up from low latitudes, and in circulating around the anticyclone, the parcels in the region of the low-ozone pocket are among those that experience the strongest diabatic descent [*Manney et al.*, 1994b].

Figure 1 summarizes the behavior of ozone at the parcel positions for the length of the back trajectory calculations. The average, minimum, and maximum observed ozone mixing ratios at the parcel positions are plotted as a function of time. The slopes for the averages shown in Figure 1, calculated using a least squares fit over the 22 days, are given in Table 1. Ozone in each case decreases at an average rate of ≈1.5-2.0%/d for the ensemble of parcels. As an indication of the reliability of the three-dimensional trajectory calcula-

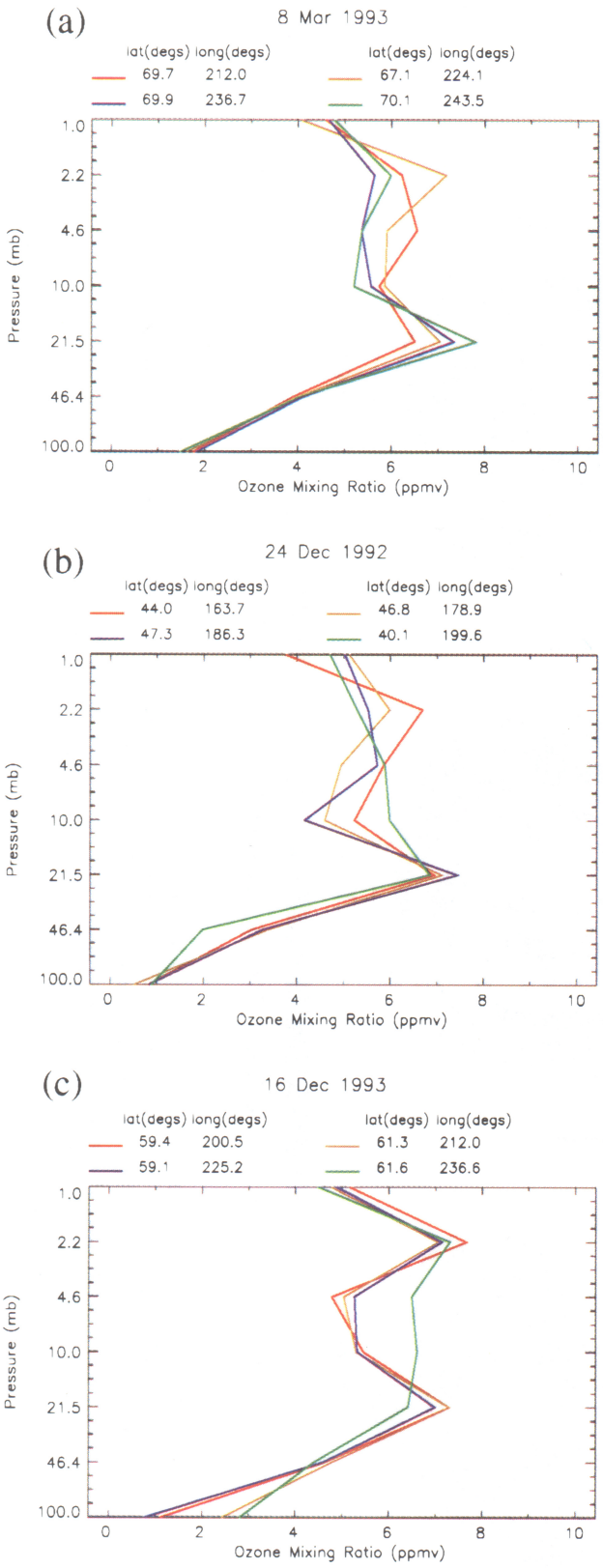

Plate 3. Individual Microwave Limb Sounder (MLS) ozone profiles on (a) March 8, 1993, (b) December 24, 1992, and (c) December 16, 1993, in the region of low ozone.

tion, the same calculation has been done for the February/March 1993 and December 1992 cases using MLS H_2O, CLAES N_2O, and CLAES CH_4. Figure 2 shows the results for N_2O, and the least squares fits for each of the tracers are given in Table 1. The N_2O values for February/March 1993 show little trend (Figure 2a), with the uncertainty being about half the magnitude of the slope; the slopes for the other passive tracers are also relatively small during this period. This is in contrast to the ozone (Figure 1a), which shows a steady decreasing trend of ≈2%/d. The slopes for the tracers in December 1992 are again much smaller than those for ozone. The N_2O values for December 1992 show a greater trend than was apparent for February/March 1993 when averaged over the 22-day period. However, most of the change occurs around December 14-16 (Figure 2b); when the periods before and after this are fitted separately, the slopes for N_2O are only ≈0.3%/d, while those for ozone remain near 1.5%/d. 14-16 December is approximately the time before which the parcels split into two general groups (see Plate 4d), and this may indicate a greater uncertainty in the trajectory calculations for days before ≈December 14.

The passive tracer calculations suggest that the trajectory code can fairly accurately reproduce the air motion. The behavior of the tracers is in contrast to the steady, consistent downward trend in ozone at the parcel positions in each case. In February/March 1993 the average ozone mixing ratio closely parallels the maximum; the low minimum values result from a few (of the order of 10 out of 3200) parcels that end up away from the others, as seen in Plate 4b. In each case, the average value on the earliest day is greater than the maximum value on the initialization day.

Plate 6 shows the average of the ozone profiles at the horizontal postions of the parcels started at 840 K (the ozone profile is interpolated to each parcel's latitude and longitude, and then the values at each level are averaged) as a function of potential temperature on each day of the trajectory calculations. The average potential temperature of the ensemble of parcels that started at 840 K is also indicated. The same kind of plots for parcels started at 740 and 960 K are very similar to Plate 6, suggesting that the horizontal motions are similar over a relatively deep vertical range. Although Plate 6 does not show the exact environment through which the parcels move (because of the vertical shear), the horizontal motions are sufficiently similar over a deep vertical range that these average profiles should give a reasonable approximation to that environment.

At the end of the back trajectory calculation, ozone mixing ratios as low as those at the initial (latest day) parcel potential temperature are seen only several hundred Kelvin above or below the parcel potential temperature. This suggests that the calculated potential temperature would have to be in error by several hundred Kelvin in order to obtain the observed mixing ratio by vertical transport, if the average calculated horizontal motion is accurate. An error of this magnitude is not expected in the radiation calculation for the mid-

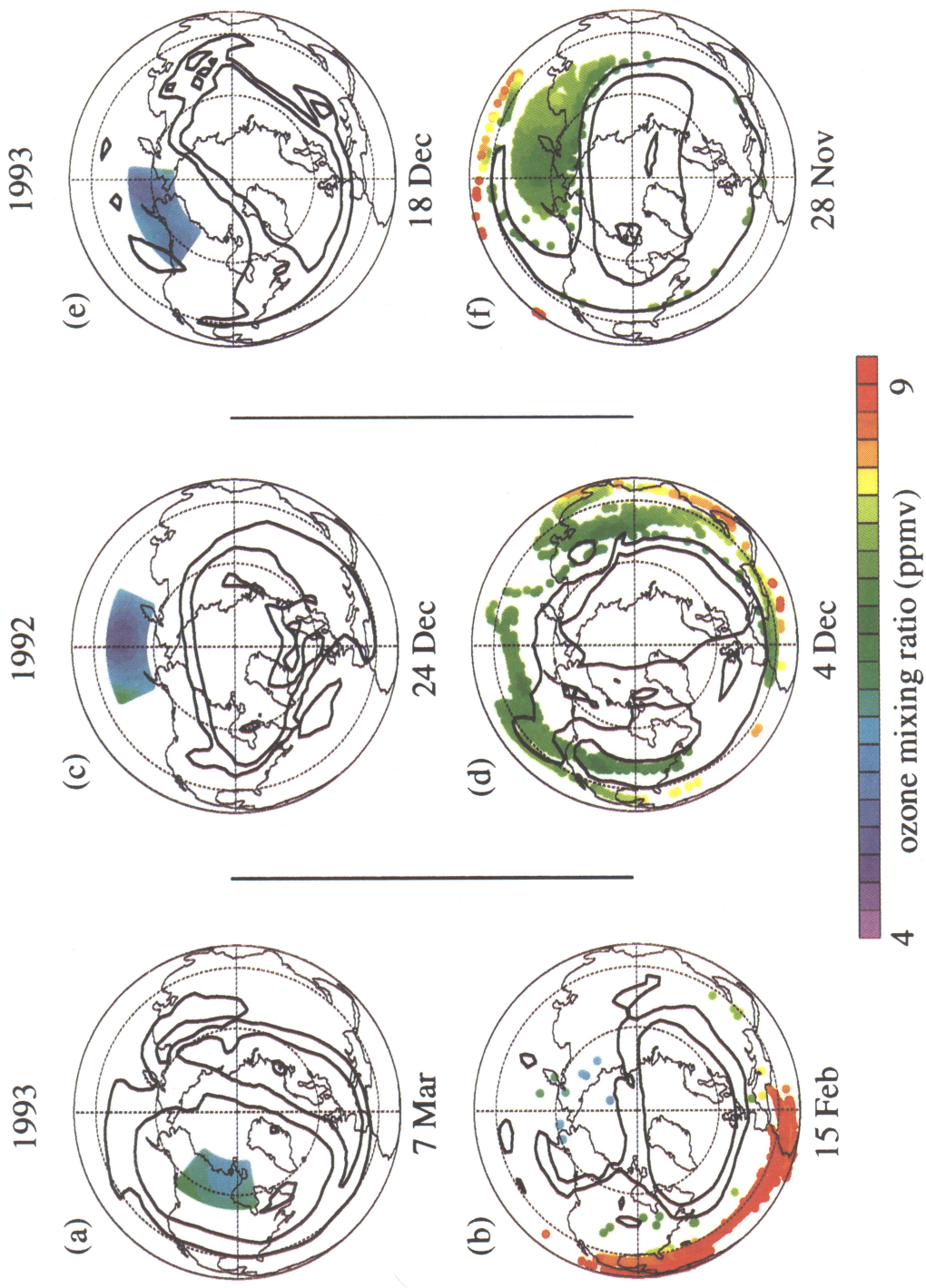

Plate 4. Initial horizontal positions of parcels started at 840 K on (a) March 7, 1993, (c) December 24, 1992; and (e) December 18, 1993, and the positions of those parcels 20 days previously (b, d, and f). Parcels are color coded by the observed ozone value at their position on the plotted day. Projection is orthographic, with 0° longitude at the bottom of the plot, and 30° and 60° latitude circles shown as thin dashed lines. The same 840 K PV contours shown in Plate 1 are overlaid.

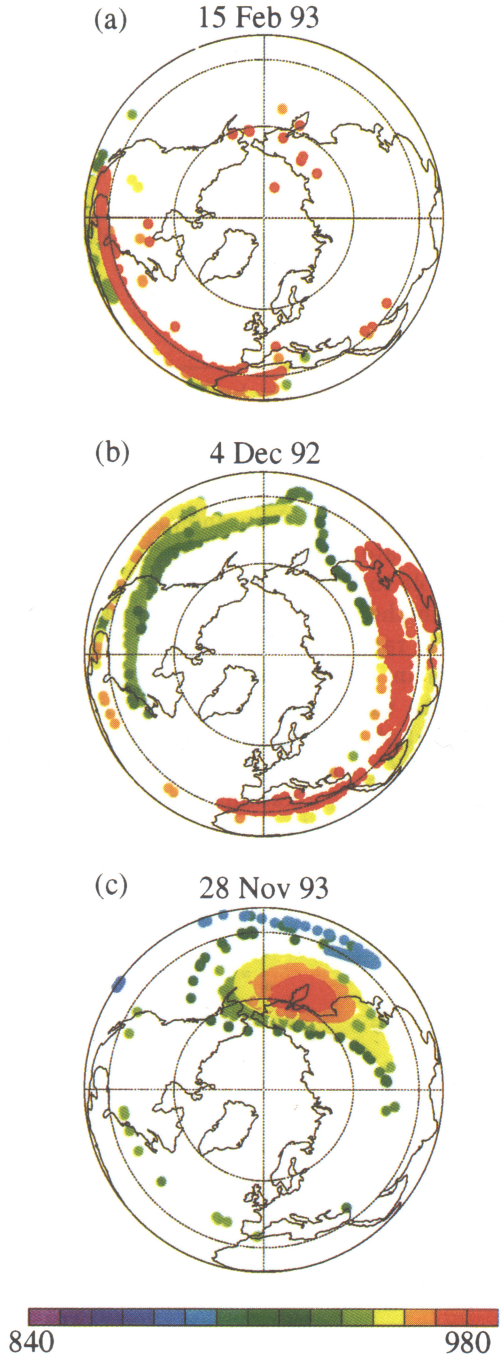

Plate 5. As in Plate 4, for 20 days prior to initialization only, and with parcels color coded by their potential temperature.

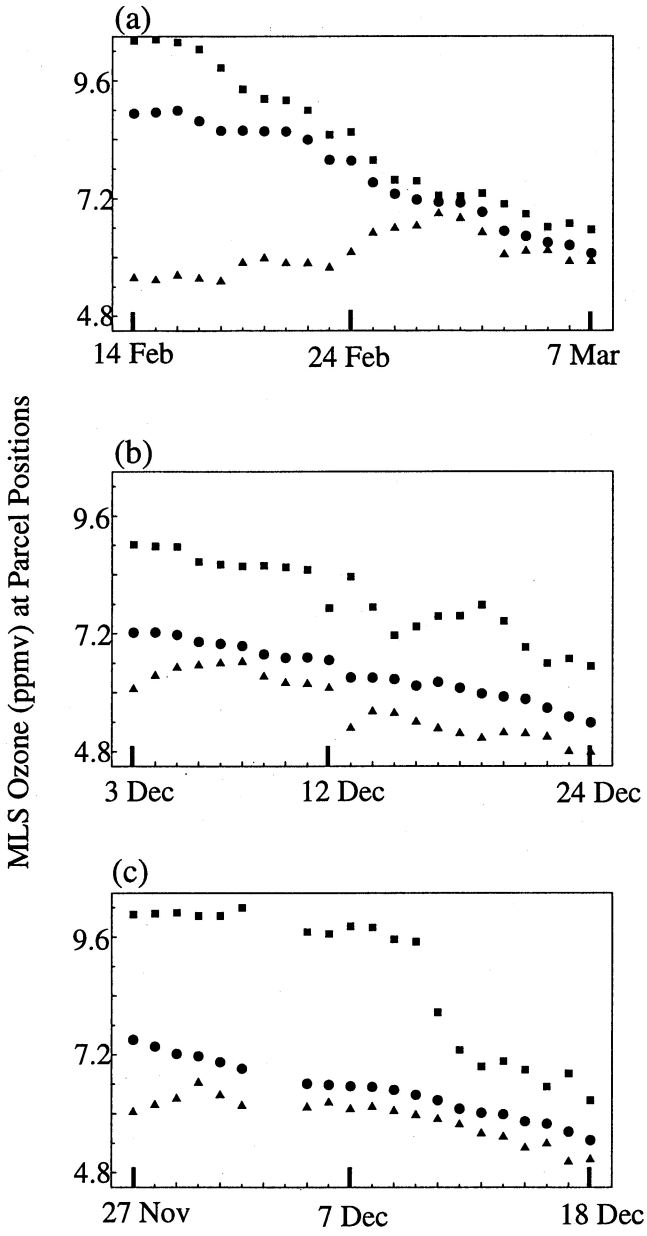

Figure 1. Average (circles), minimum (triangles) and maximum (squares) ozone mixing ratio (ppmv) at parcel positions on each day of the back trajectory calculation for (a) February/March 1993, (b) December 1992, and (c) December 1993. Figures 1a and 1b are averaged over 3200 parcels and Figure 1c over 3840 parcels.

stratosphere. Plots of N_2O similar to Plate 6 show that the dots representing the average parcel potential temperature closely follow an N_2O contour, indicating that the calculation of vertical motion is reasonably accurate. In addition, sensitivity tests were done for the February/March 1993 case by running the trajectory calculation, but with diabatic cooling rates increased or decreased by 40%. These tests show that even if the diabatic cooling was 40% stronger or weaker than that calculated here, the parcels would still have come from a low-latitude region of much higher ozone.

The results in this section indicate that the observed pockets of low ozone in the midstratospheric anticyclone could not result from transport processes alone.

Discussion

Three examples are shown of the formation of an isolated region of low ozone mixing ratios in the NH anticyclone during strong stratospheric warmings. These examples are typical of the ozone behavior in the midstratosphere when a strong anticyclone develops. In addition to the examples given here, a similar pocket of

Table 1. Time Rates of Change of Average O_3, N_2O, CH_4, and H_2O at Positions of Parcels Started at 840 K

Time Period	$\Delta O_3/\Delta t$ ppmv/d	$\Delta N_2O/\Delta t$ ppbv/d	$\Delta CH_4/\Delta t$ ppmv/d	$\Delta H_2O/\Delta t$ ppmv/d
Feb./March 1993	-0.152 ± 0.006 (-2.3%/d)	-0.44 ± 0.22 (-0.4%/d)	-0.010 ± 0.003 (-0.8%/d)	-0.31 ± 0.004 (-0.6%/d)
Dec. 1992	-0.086 ± 0.003 (-1.5%/d)	0.51 ± 0.10 (0.6%/d)	-0.006 ± 0.002 (-0.5%/d)	-0.31 ± 0.002 (-0.6%/d)
Dec. 1993	-0.088 ± 0.002 (-1.5%/d)			

Time rates of change are calculated using a linear least squares fit over the 22 days of the back trajectory calculation. Approximate changes in percent per day are given in parentheses.

low ozone forms in the anticyclone during every strong NH warming observed by MLS. Since SH warmings are generally much weaker than in the NH, and any SH anticyclone that forms is usually a very transient feature, examples of this type of behavior are less frequent in the SH. However, Plate 7 shows 840 K SH ozone on August 22, 1993, and on May 30, 1994, each a few days after the peak of a SH warming when an anticyclone had formed. There is a suggestion of a region of low ozone in the anticyclone on August 22, 1993, and a distinct pocket of low ozone in the anticyclone on May 30, 1994. Vertical profiles in these regions (Plate 8) show a bite out of the profiles similar to but smaller than those seen in the NH. May 30, 1994 is only a few days after MLS began observing the SH, so no back trajectories were computed for this case. Plate 9 shows observed ozone at parcel positions on August 22, 1993 (the initial day) and 13 days earlier (the first day MLS was looking south). While not so dramatic as the NH examples, the calculation does show the parcels originating from low-latitude regions of higher ozone, and average ozone at the parcel positions decreases at ≈1%/d over the period. An analysis similar to that described in the discussion of Plate 6 suggests that the calculated vertical position of the parcels would have to be in error by ≈100 K in potential temperature over the 14 days in order to produce the observed ozone on August 22 solely by transport processes. Thus the same phenomenon described for the NH does in fact occur in the SH when the anticyclone becomes sufficiently strong and persistent.

Although the formation of low-ozone pockets in the anticyclone has not been previously studied in detail, the phenomenon is apparent in midstratospheric limb infrared monitor of the stratosphere (LIMS) data shown by *Leovy et al.* [1985]. Plate 10 Shows 840 K LIMS ozone on January 23, 1979, during a strong warming. A low-ozone region similar to those studied here is apparent in the anticyclone. This bite out of the LIMS ozone profiles extends vertically from ≈20 to 7 hPa. It appears that this feature may not be so intense as some of those seen in MLS observations, but the separation of over a decade between the two data sets and the limited length of the LIMS data set render such comparisons speculative.

Rood et al. [1993] noted an anomaly in LIMS nitric acid (HNO_3) in late January 1979, with high HNO_3 values, comparable to those in the polar vortex, in an isolated region in the anticyclone. This feature was seen over a vertical range from ≈30 to 5 hPa. The ozone pocket shown in Plate 10 is nearly coincident in the horizontal with the HNO_3 anomaly reported by *Rood et al.* [1993], but is apparent only between ≈20 and 7 hPa. The HNO_3 anomaly is slightly downstream of the low-ozone region. Examination of CLAES HNO_3 data during February/March 1993 and December 1992

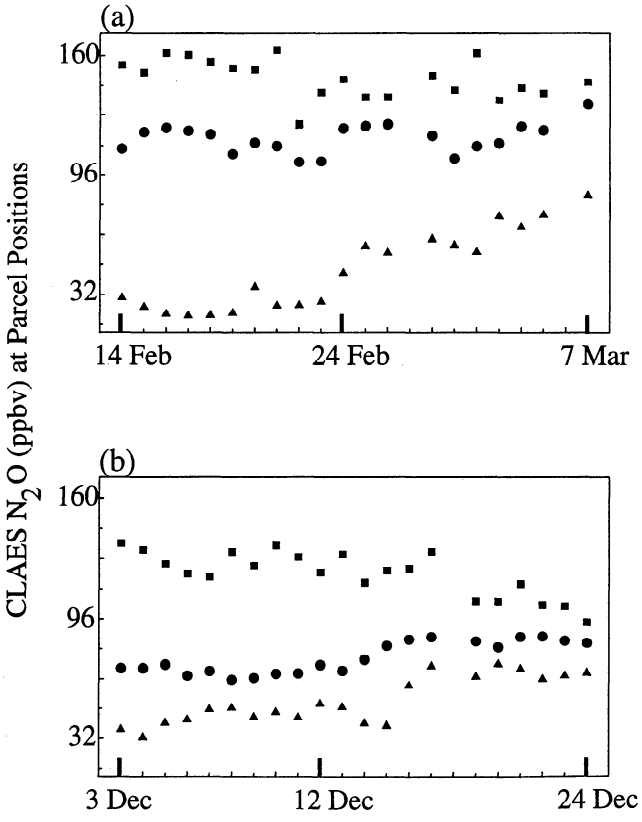

Figure 2. As in Figure 1 but for nitrous oxide (N_2O) mixing ratio (parts per billion by volume (ppbv)), and for (a) February/March 1993 and (b) December 1992 only.

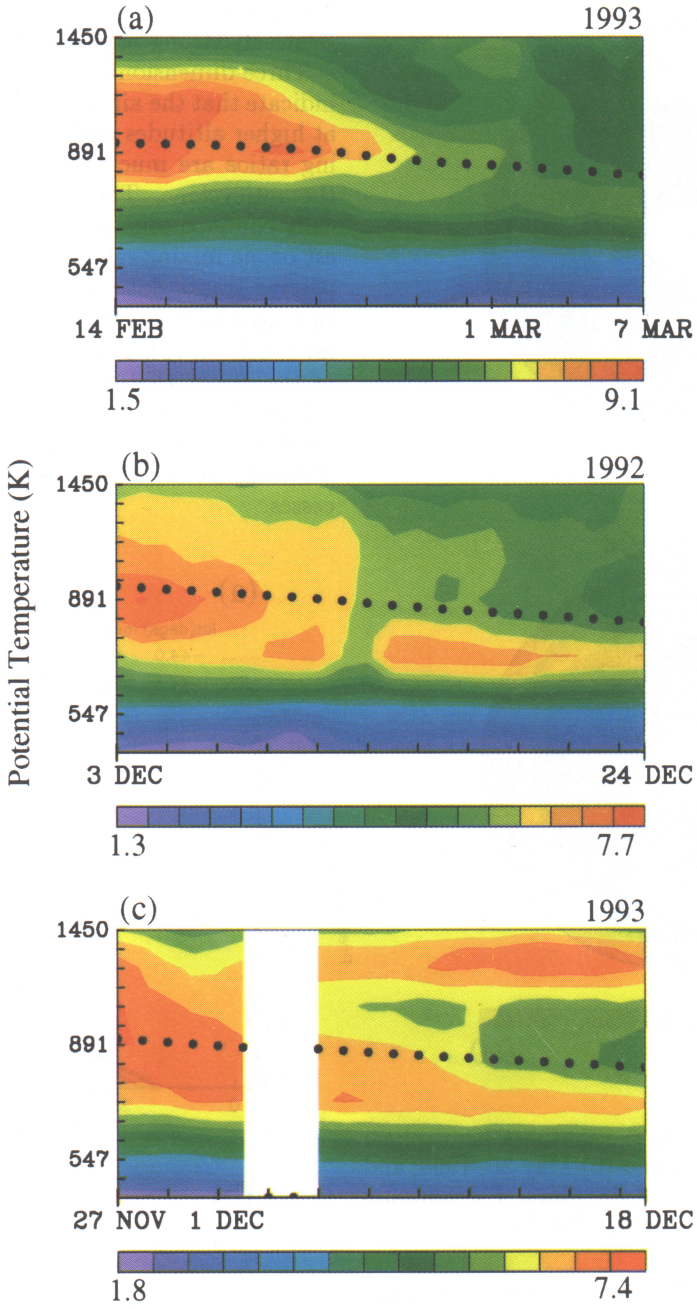

Plate 6. Average ozone (ppmv) profile at horizontal positions of parcels initialized at 840 K. Ozone is interpolated to each parcel's latitude and longitude at each level and then the profiles are averaged. For (a) February/March 1993, (b) December 1992, and (c) December 1993.

indicates that at those times there is also a region of high HNO_3 just downstream of the region of low ozone. High HNO_3 in the anticyclone was also observed by the Improved Stratospheric and Mesospheric Sounder (ISAMS) during the January 1992 nearly major stratospheric warming, when MLS also observed a pocket of low ozone (J. Remedios, manuscript in preparation, 1995). *Rood et al.* [1993] were unable to reproduce the HNO_3 anomaly observed in LIMS data using a three-dimensional chemical-transport model and concluded on that basis that there must either be serious flaws in the data or deficiencies in the chemical model. Recent independent data indicate that this phenomenon is in fact a real atmospheric feature and that it may be related to the low-ozone features described here. Work is now in progress by several groups with the goal of reproducing these phenomena in chemical models. It is not clear at present whether changes in the model chemistry will be required to explain these features, or whether a better specification of the inputs to the models and the

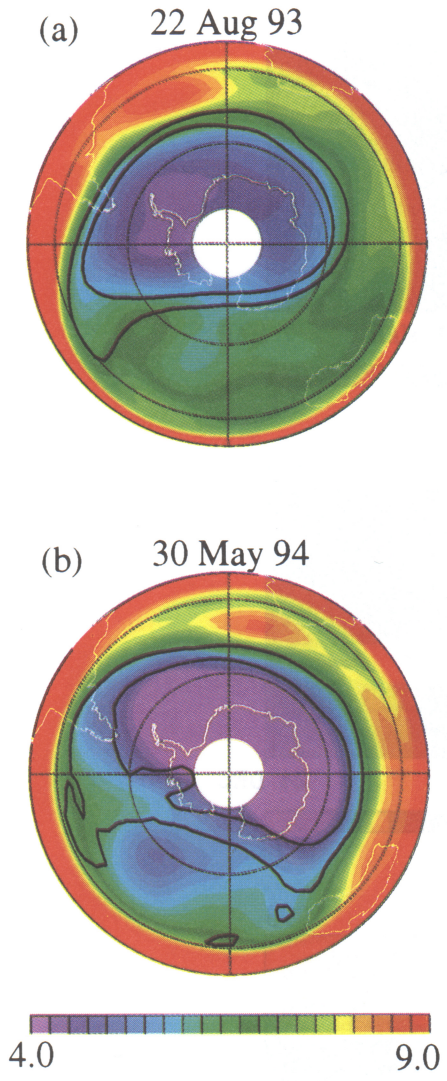

Plate 7. As in Plate 1 but for the southern hemisphere (SH) on (a) August 22, 1993 and (b) May 30, 1994, and with 0° longitude at the top of the plots. PV contours are -3.0 and -5.0×10^{-4} K m^2 kg^{-1} s^{-1}.

environment in which the low-ozone pockets form may show that they can be quantitatively reproduced using current models.

Conclusions

MLS observations of the evolution of midstratospheric ozone during stratospheric warmings have been examined during winter in each hemisphere. During warmings, tongues of high ozone are drawn up from low latitudes into the developing anticyclone. Several days later, an isolated region of low ozone mixing ratios appears, centered in the anticyclone and prominent at MLS retrieval levels of 10 and 4.6 hPa. Ozone mixing ratios in this region during NH warmings are comparable to values well inside the vortex and are typically ≈3 ppmv lower than typical midlatitude extravortex mixing ratios. This type of feature appears whenever the anticyclone is strong and persistent, including during relatively strong minor warmings in the SH.

Three-dimensional trajectory calculations shown here indicate that the air in the region of low ozone originates at higher altitudes and low latitudes, where ozone mixing ratios are much higher than those that appear in the anticyclone. The air parcels studied here are typically confined together for 1 to 3 weeks before the lowest ozone mixing ratios are observed. Comparison with passive tracer data shows that the trajectory calculation used here can fairly accurately reproduce observed air motions. This and the extremely large magnitude of the errors that would be implied in the trajectory calculation to get observed ozone values by transport confirm that the observed low-ozone pockets in the midstratosphere could not result solely from transport processes.

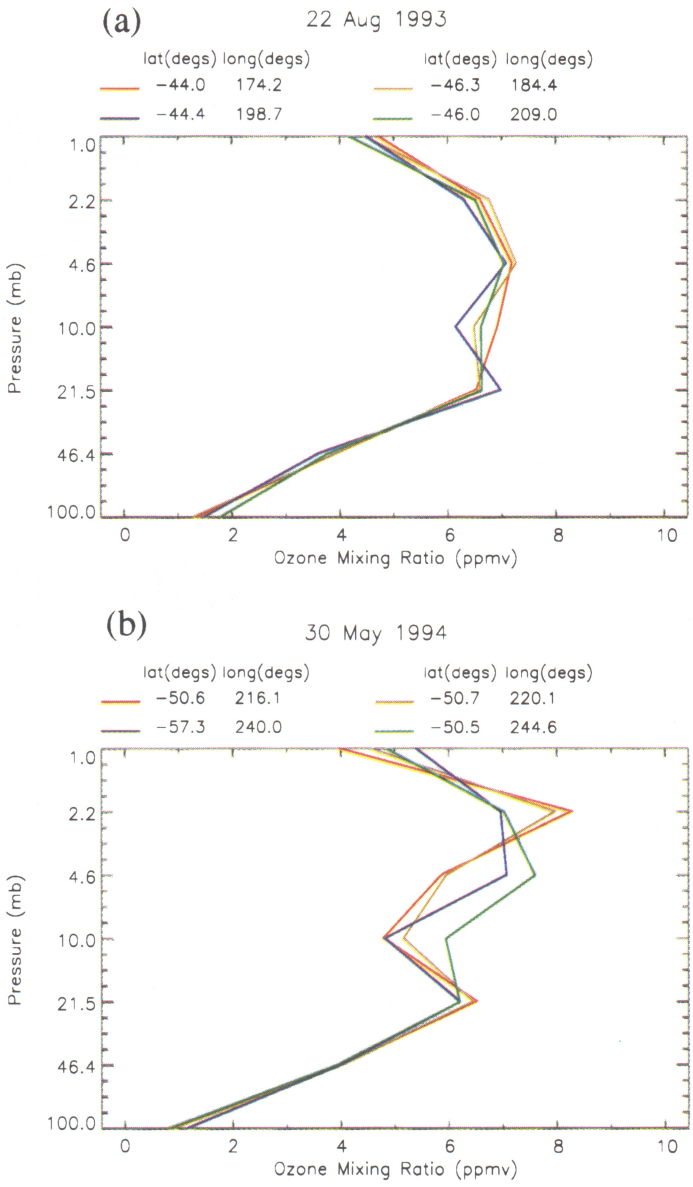

Plate 8. As in Plate 3 but for (a) August 22, 1993, and (b) May 30, 1994 in the SH.

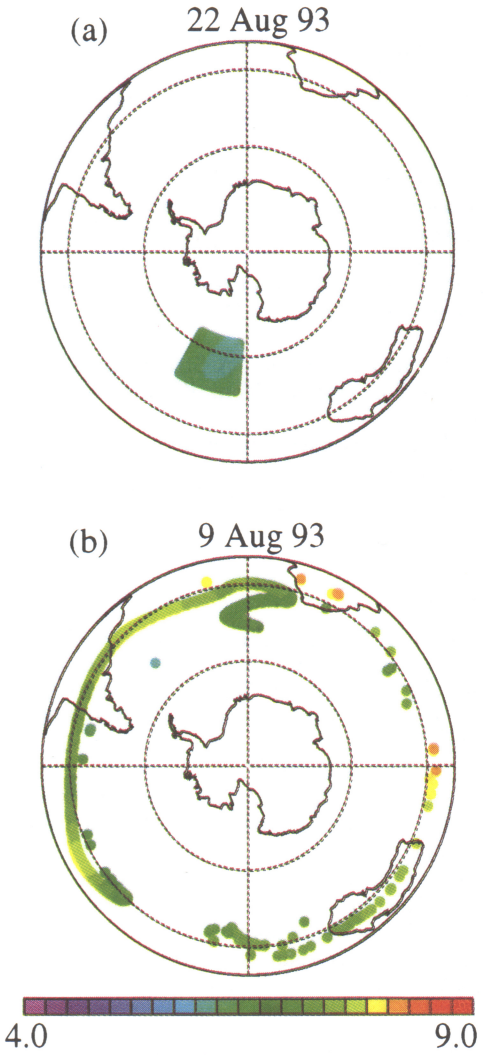

Plate 9. As in Plate 4 but for a back trajectory run started August 22, 1993, in the SH, on the initial day and 13 days previously. 0° longitude is at the top of the plots.

Several modeling investigations are under way, aimed at understanding the chemical processes involved in the formation of these low ozone regions. The following summarizes the features that must be explained by combined chemical and dynamical models:

1. Low ozone appears in the anticyclone several days after the peak of a stratospheric warming.
2. The low-ozone pocket extends from ≈15 to 5 hPa in the vertical, with higher ozone above and below.
3. The region of low ozone is downstream (eastward and equatorward) of the region of maximum temperature.
4. The air in which the low ozone appears originates at low latitudes and higher altitudes, in regions of much higher ozone.

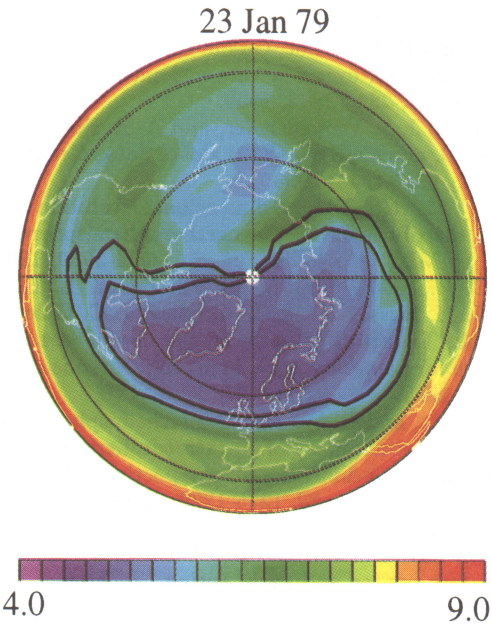

Plate 10. As in Plate 1 but for January 23, 1979, from limb infrared monitor of the stratosphere data.

5. This air remains localized together for 1 to 3 weeks prior to the appearance of minimum ozone mixing ratios.
6. Anomalies in HNO_3 [*Rood et al.*, 1993] and possibly other species (J. Remedios, manuscript in preparation, 1995) are observed concurrently.

Acknowledgments. Thanks to our MLS and CLAES colleagues for their contributions to its success; to B. Ridenoure for data analysis and graphics assistance, to T. Luu for data management, and to P. Newman for supplying routines that were adapted to calculate PV. The UARS investigations at the Jet Propulsion Laboratory, California Institute of Technology were carried out under contract with the National Aeronautics and Space Administration.

References

Andrews, D. G., J. R. Holton, and C. B. Leovy, *Middle Atmosphere Dynamics,* 489 pp., Academic Press, San Diego, Calif., 1987.

Barath, F. T., et al., The Upper Atmosphere Research Satellite microwave limb sounder instrument, *J. Geophys. Res., 98,* 10,751-10,762, 1993.

Elson, L. S., and L. Froidevaux, The use of Fourier transforms for asynoptic mapping: Early results from the Upper Atmosphere Research Satellite microwave limb sounder, *J. Geophys. Res., 98,* 23,039-23,049, 1993.

Farrara, J. D., M. Fisher, C. R. Mechoso, and A. O'Neill, Planetary-scale disturbances in the southern stratosphere during early winter, *J. Atmos. Sci., 49,* 1757-1775, 1992.

Fishbein, E. F., L. S. Elson. L. Froidevaux, G. L. Manney, W. G. Read, J. W. Waters, and R. W. Zurek, MLS observations of stratospheric waves in temperature and ozone during the 1992 southern winter, *Geophys. Res. Lett., 20,* 1255-1258, 1993.

Froidevaux, L., J. W. Waters, W. G. Read, L. S. Elson, D. A. Flower, and R. F. Jarnot, Global ozone observations from UARS MLS: An overview of zonal mean results, *J. Atmos. Sci., 51,* 2846-2866, 1994.

Kumer, J. B., J. L. Mergenthaler, and A. E. Roche, CLAES CH_4, N_2O, and CCL_2F_2 (F12) global data, *Geophys. Res. Lett., 20,* 1239-1242, 1993.

Lahoz, W. A., et al., Three-dimensional evolution of water vapour distributions in the northern hemisphere as observed by MLS, *J. Atmos. Sci., 51,* 2914-2930, 1994.

Leovy, C. B., C.-R. Sun, M. H. Hitchman, E. E. Remsberg, J. M. Russell III, L. L. Gordley, J. C. Gille, and L. V. Lyjak, Transport of ozone in the middle stratosphere: Evidence for planetary wave breaking, *J. Atmos. Sci., 42,* 230-244, 1985.

Manney, G. L., and R. W. Zurek, Interhemispheric comparison of the development of the stratospheric polar vortex during fall: A 3-dimensional perspective for 1991-1992, *Geophys. Res. Lett., 20,* 1275-1278, 1993.

Manney, G. L., J. D. Farrara, and C. R. Mechoso, The behavior of wave 2 in the Southern Hemisphere stratosphere during late winter and early spring, *J. Atmos. Sci., 48,* 976-998, 1991.

Manney, G. L., L. Froidevaux, J. W. Waters, L. S. Elson, E. F. Fishbein, R. W. Zurek, R. S. Harwood, and W. A. Lahoz, The evolution of ozone observed by UARS MLS in the 1992 late winter southern polar vortex, *Geophys. Res. Lett., 20,* 1279-1282, 1993.

Manney, G. L., R. W. Zurek, A. O'Neill, R. Swinbank, J. B. Kumer, J. L. Mergenthaler, and A. E. Roche, Stratospheric warmings during February and March 1993, *Geophys. Res. Lett., 21,* 813-816, 1994a.

Manney, G. L., R. W. Zurek, A. O'Neill, and R. Swinbank, On the motion of air through the stratospheric polar vortex, *J. Atmos. Sci., 51,* 2973-2994, 1994b.

Remsberg, E. E., P. P. Bhatt, and T. Miles, An assessment of satellite temperature distributions used to derive the net diabatic transport for zonally averaged models of the middle atmosphere, *J. Geophys. Res., 99,* 23,001-23,030, 1994.

Roche, A. E., J. B. Kumer, J. L. Mergenthaler, G. A. Ely, W. G. Uplinger, J. F. Potter, T. C. James, and L. W. Sterritt, The cryogenic limb array etalon spectrometer (CLAES) on UARS: experiment description and performance, *J. Geophys. Res., 98,* 10,763-10,775, 1993.

Rood, R. B., A. R. Douglass, J. A. Kaye, and D. B. Considine, Characteristics of wintertime and autumn nitric acid chemistry as defined by Limb Infrared Monitor of the Stratosphere (LIMS) data, *J. Geophys. Res., 98,* 18,533-18,545, 1993.

Shine, K. P., The middle atmosphere in the absence of dynamic heat fluxes, *Q. J. R. Meteorol. Soc., 113,* 603-633, 1987.

Swinbank, R., and A. O'Neill, A Stratosphere-troposphere data assimilation system, *Mon. Weather Rev., 122,* 686-702, 1994.

Waters, J. W., Microwave limb sounding, in *Atmospheric Remote Sensing by Microwave Radiometry,* edited by M. A. Janssen, pp. 383-496, Wiley, New York, 1993.

L. Froidevaux, G. L. Manney (corresponding author), J. W. Waters, and R. W. Zurek, Jet Propulsion Laboratory/California Institute of Technology, 4800 Oak Grove Drive, Mail Stop 183-701, Pasadena, CA 91109-8099.

J. C. Gille, National Center for Atmospheric Research, P.O. 3000, Boulder, CO 80307.

J. B. Kumer, J. L. Mergenthaler, and A. E. Roche, Lockheed Palo Alto Research Laboratory, 3251 Hanover St., Palo Alto, CA 94304.

A. O'Neill, Centre for Global Atmospheric Moddelling, University of Reading, 2 Earley Gate, Whiteknights, Reading RG6 2AU United Kingdom.

R. Swinbank, CR Division, Meteorological Office, London Road, Bracknell RG12 2SZ United Kingdom.

(Received August 22, 1994; accepted January 21, 1995.)